Operational Boundaries on the Stellarator W7-AS at the Beginning of the Divertor Experiments

R. Jaenicke, M. Anton, J. Baldzuhn, S. Bäumel, R. Brakel, R. Burhenn, H. Callaghan, G. Cattanei, D. Dorst, H. Ehmler, A. Elsner, M. Endler, V. Erckmann, Y. Feng, S. Fiedler, C. Fuchs, F. Gadelmeier, J. Geiger, L. Giannone, P. Grigull, H. Hacker, H.J. Hartfuß, D. Hartmann, D. Hildebrandt, M. Hirsch, E. Holzhauer, F. Karger, M. Kick, J. Kisslinger, S. Klose, J.P. Knauer, J.P. Koponen, R. Koenig, G. Kühner, H. Laqua, L. Ledl, H. Maaßberg, H. Niedermeyer, K. McCormick, D. Naujoks, W. Ott, F.-P. Penningsfeld, S. Reimbold, N. Ruhs, N. Rust, J. Saffert, E. Sallander, J. Sallander, F. Sardei, M. Schubert, E. Speth, U. Stroth, F. Volpe, F. Wagner, A. Weller, Chr. Wendland, A. Werner, E. Würsching

Max-Planck- Institut fuer Plasmaphysik, EURATOM Association, 85748 Garching, Germany

e-mail contact of main author: jaenicke@ipp.mpg.de

Abstract. During the last shutdown the Stellarator W7-AS underwent two major modifications: First, the limiters were replaced by ten divertor modules, and the diagnostic set associated with the plasma boundary and target plate regions was greatly expanded. Secondly, the previously counter tangential neutral beam injector box was shifted to a co-position. Thus, the heating efficiency should be considerably increased at low magnetic fields and high densities. After resuming experiments these improvements will be used to test the boundary island divertor concept and further expand operational boundaries during the remaining experimental time until permanent shutdown in 2002. The present operational boundaries are reviewed with respect to the stability of high β and density limit discharges. Discharges with good confinement properties will be discussed where further progress was achieved after installing control coils to modify the size and properties of vacuum field islands. In contrast to the usual net-current free mode, W7-AS also allows operation at large toroidal currents. In this way disruption-like events in the presence of rather large external poloidal fields can be produced.

1. Introduction

The stellarator line of IPP concentrates on low shear devices, which allow exclusion of resonances with low order rational numbers n/m = 1/3, 1/2,... from the confinement region and provide stability by a magnetic well rather than by strong shear. A typical representative of this concept was W7-A, where the flux surfaces were produced by toroidal field coils together with an l=2, m=5 helical winding. However, this classical stellarator approach has enhanced neoclassical transport by trapped particles, and the β-limit is too low for an economic fusion reactor. The pressure driven bootstrap current generates a significant contribution to the total rotational transform and thus contradicts the concept that the magnetic configuration can be controlled by external currents alone. It is concluded from these arguments that this classical stellarator concept needs to be optimized [1,2].

W7-AS [1,3] is a first step on the way to such an optimized stellarator. Its magnetic field is generated by modular twisted coils, which carry both the required helical and toroidal current components. The toroidal and vertical field coils are just for experimental flexibility. The OH transformer is commonly used to compensate toroidal currents, such as the bootstrap current (tokamak-like on W7-AS), to zero, this being called "net-current-free" operation. The plasma cross-section varies toroidally between a rather triangular shape and an almost elliptical shape [1]. The magnetic axis is not circular, but rather pentagonal in keeping with the 5 toroidal field periods. W7-AS was designed to test two improvements:

- the generation of closed flux surfaces by (normal conducting) modular field coils [4]
- the reduction of the Pfirsch-Schlüter (PS) currents and their effect on the plasma behaviour, especially on equilibrium and stability and on neoclassical transport.

The successor W7-X [5], presently being built in Greifswald in northern Germany, is intended to demonstrate the suitability of the optimized stellarator concept as a steady state fusion reactor. Improved numerical tools are used to optimize the magnetic field properties in three dimensions so that the major fusion plasma parameters subject to classical physics should be reached simultaneously. In addition, a plasma produced in such an optimized magnetic field configuration must not change the magnetic flux surfaces significantly. For the optimization the following set of criteria was employed [1,2]:

1) high quality of vacuum field magnetic surfaces: only small islands allowed
2) PS-currents further reduced: small Shafranov shift, high equilibrium β
3) high stability β: $<\beta> \approx 5\%$ should be achievable
4) sufficiently small neoclassical transport in the lmfp regime
5) minimized bootstrap current
6) good confinement of hot α particles in the reactor extrapolation
7) good modular coil feasibility and inherent divertor properties

These optimization criteria do not contradict each other and can in fact be satisfied simultaneously, if some compromises are accepted.

The main task of W7-AS was and is to verify the predictions of the optimization procedure as far as possible by experiments [6]. In the past it has been demonstrated that the PS currents are reduced as expected [1,7], and that neoclassical transport can be described by the 3D DKES code including the important trapped particle effects and radial electric fields in the long mean free path (lmfp) regime [8]. Consequently, predictions for W7-X, where neoclassical transport must be strongly reduced, have a solid foundation. Bootstrap currents can be measured rather easily and agree with theoretical predictions within a factor 2 where experimental uncertainties in profiles, Z_{eff} etc. also have to be taken into account [9]. Maximum $<\beta>$-values close to 2% were achieved with maximum neutral beam (NB) heating power at very high densities of about $2 \cdot 10^{14}$ cm^{-3}. They are determined by a slow radiative decay; no violent MHD processes are observed. Thus, maximum $<\beta>$-values are limited by the available heating power at given radiation losses.

On the other hand, experiments with high NB heating power demonstrate very clearly that a divertor is needed to improve the insufficient density and impurity control and to reduce the high local heat loads on limiters. Therefore, during the shutdown in 1999/2000 all limiters have been replaced by ten divertor modules, with the aim to perform extensive tests of the island divertor concept foreseen for W7-X. At the same time the (previously counter) tangential NB injector box has been shifted to a co-position, leading to an augmented heating efficiency at low magnetic fields and at high densities. These improvements will allow W7-AS to expand operational boundaries during the remaining experimental time.

The present operational boundaries are reviewed with respect to the stability of high β and density limit discharges (Section 2 and 3) and with respect to high confinement where further progress was achieved after installing control coils to modify the size and properties of vacuum field islands (Section 5). The preparation of island divertor experiments is discussed in Section 4. New H-mode results are presented in Section 6. Finally, disruption-like events in the case of finite toroidal currents are addressed in Section 7. Results on recent progress with ICRH, ECRH and electron cyclotron current drive (ECCD) can be found in Refs.[10-12].

2. Stability at high β

The predicted high β stability was an important criterion for the choice of the W7-X magnetic field configuration. Thus high β-limits were carefully checked on W7-AS to obtain experimental information on the reliability of theoretical predictions, although the achievable temperature and β-values are quite different. Whereas for W7-X ideal and resistive interchange as well as ideal ballooning modes are expected to be stable up to $<\beta> \approx 5\%$ [see e.g. 1,13], resistive interchange modes are predicted unstable below the experimentally achieved $<\beta>$-values on W7-AS, especially in configurations with high vertical fields where the magnetic well is strongly reduced [14]. A more detailed stability analysis compared with experimental results will be published in Ref. [15].

Experimentally, maximum β-values ($<\beta> \approx 2\%$ or $\beta(0) < 4.5\%$) were obtained at a toroidal field of $B_o \approx 1.25$ T and at densities of about $2 \cdot 10^{14}$ cm^{-3} with balanced 2.5 MW NB heating (4 co- and 4 counter-sources). They are limited by a slow radiative decay with no violent MHD processes being observed [16]. Also the equilibrium β-limit imposes no serious problem, although the Shafranov shift is large [17]. It is large due to the large aspect ratio and the small rotational transform $\iota > 1/3$ and reduced by an optimization factor of just 2. Thus, up to now maximum $<\beta>$-values are determined by the available heating power at given radiation losses. At still lower B_o $<\beta>$-values remained almost constant, because the heating efficiency of the counter sources decreases considerably. The deviations of the 50 keV ion drift surfaces from the flux surfaces are large compared with the rather small plasma radius of about 17 cm and are directed to the plasma boundary for counter injection. In addition, at high density the fast ions are born preferentially at large plasma radii. The resulting different heating efficiencies of co- and counter sources are predicted by Monte-Carlo codes [18] and have been demonstrated experimentally (Fig. 1).

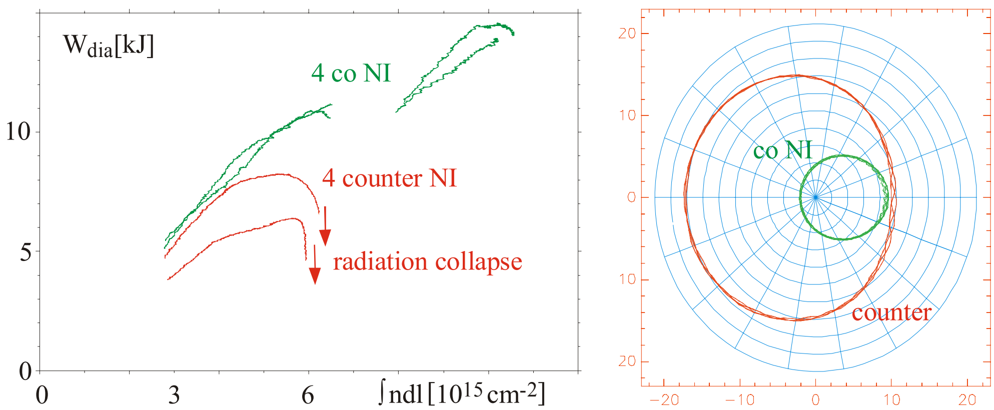

Fig. 1. Heating efficiency of co- and counter NB sources. Left: discharges with only counter NI suffer from a radiation collapse at rather low densities, whereas discharges with only co NI allow much higher densities and lead to much higher energy contents (B_o = 1.25 T, ι = 0.35). Right: calculated gyro-center orbits for 50 keV ions in magnetic coordinates at B_o = 1.7 T and ι = 0.40. The large deviation of the drift surfaces causes considerable hot ion losses in the case of counter injected ions.

Consequently, a rather easy method to increase the NB heating power was to "turn around" one NB injection box or shift it to another co-position. Thus, higher β-values should be accessible, offering another chance to test high β stability predictions. Another interesting aspect of powerful unbalanced NB injection will be the expected toroidal plasma rotation. However, as long as the density cannot be kept sufficiently small (potential improvement by means of divertor pumping) this rotation will be heavily damped due to the low temperatures.

3. Density Limit

The high β limit is essentially determined by the available neutral beam heating power (see Section 2) and the maximum achievable plasma density, which is a function of the heating power as well. Thus the β limit and the density limit ($\bar{n}_e \approx 2.5\ 10^{14}\ cm^{-3}$ at $B_o = 2.5T$) often coincide. Both are characterized by a slow radiation collapse where MHD instabilities do not play a significant role. However, these discharges with maximum NB heating power are not stationary at least with respect to the particle transport since density control is a substantial problem without active pumping due to the neutral beam particle fuelling. To investigate the detailed physics of the density limit, long pulses at low ECRH or NB heating power are better suited [19].

Typical examples are discharges with 350 kW NB heating power at constant line density for different pulse lengths up to 1.8 s. They demonstrate that the achievable maximum density decreases with increasing pulse duration. Due to the rising central radiation a stationary state of the impurity radiation is never reached at high densities before the central radiation power density exceeds that of the deposited power density. Thus at higher densities the radiation collapse occurs earlier. The measured impurity radiation can be simulated by a simple model of bulk radiation, and a scaling law can be derived for the maximum achievable density as a function of the volume averaged heating power p_{abs} and the toroidal field (entering as a consequence of the magnetic field dependence of the transport) [20]:

$$n_{max} \propto p_{abs}^{0.48} \cdot B_o^{0.54}$$

The existence of a density limit on W7-AS can also be demonstrated with ECRH density ramp discharges where the heating power is reduced such that the maximum density is no longer given by the cutoff density. The interesting aspect is that at some maximum density the density can no longer be raised even with stronger gas puffing. Evidently, the plasma simply does not "accept" gas coming from the outside (Fig. 2), similar to the refuelling limit observed on JET [21]. This may underline the importance of the plasma edge as it is widely accepted in tokamak models (see e.g. [22]) where the edge density is claimed to be given by the power flux through the plasma boundary which in turn is determined by the bulk impurity radiation. In that sense it will be interesting to see whether the density limit remains determined by core impurity radiation, or whether MHD instabilities will also become important in the presence

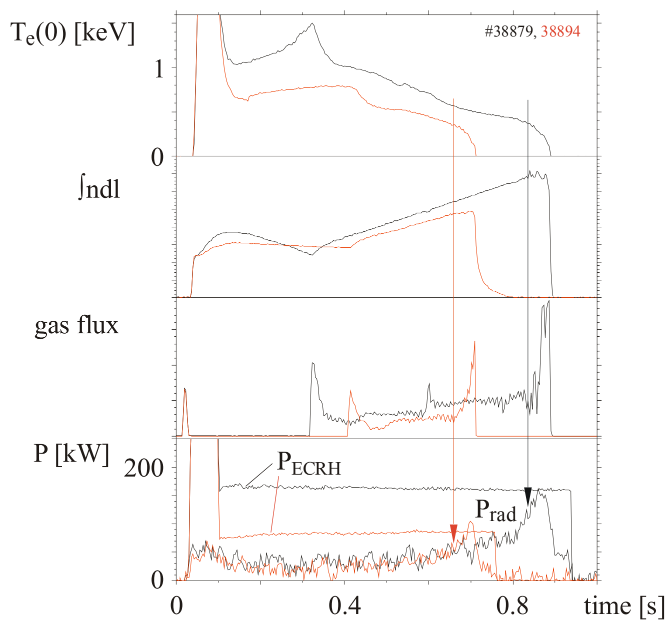

Fig. 2. Density limit discharges with low power 140 GHz ECRH. The density can be raised up to the density limit at the end of the discharge (n_e up to about 6 and $8{\cdot}10^{13}$ cm^{-3}) where the temperature drops and the radiation increases, and where the density even with strong gas puffing can no longer be elevated.

of the divertor.

4. Preparation of the Island Divertor Experiments

As mentioned in previous sections, high power NB-heated discharges on W7-AS suffer from an uncontrollable density increase and require a low impurity content. In addition, the limiter thermal load was often found to exceed the critical value of 10 MW/m^2. The non-axisymmetric stellarator offers an elegant solution for these problems via a divertor based on the use of so-called "natural islands". Such islands are an intrinsic property of non-axisymmetric flux surfaces - meaning that additional coils to produce a divertor x-point are not required. The natural islands are resonant magnetic field islands appearing for $\iota\!\!\!-$ = n/m, where n=5 is given by the 5 toroidal field periods. They can be large enough for effective divertor action. W7-X will be equipped with such an island divertor, but W7-AS already allows basic elements of this concept to be evaluated [23,24].

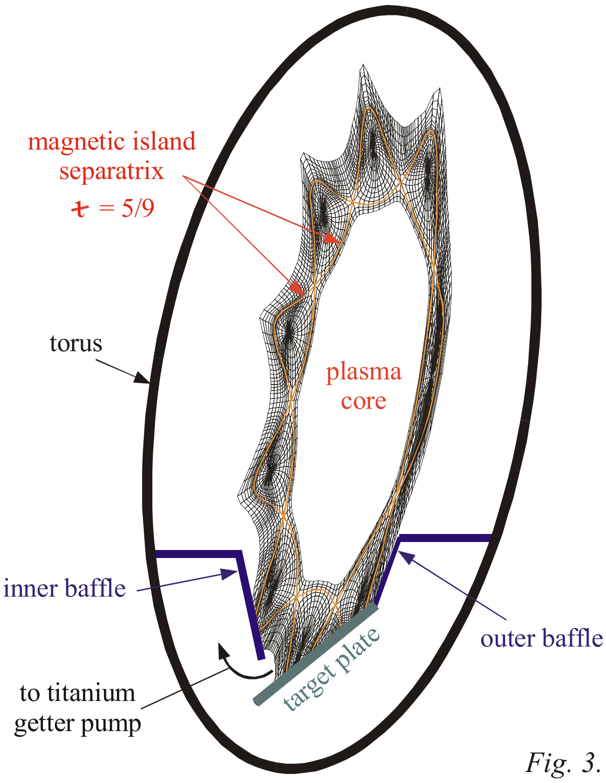

Fig. 3. Schematic view of island divertor.

A schematic view of the W7-AS island divertor is presented in Fig. 3. Ten divertor modules have been installed (2 per field period at the top and bottom of the elliptical plasma cross section). The divertor modules have to follow the 3D magnetic island structure (Fig. 4). As documented in first divertor experiments, the plasma-wall interaction indicated by the H_α emission in Fig. 5 takes place essentially on the target plates for the divertor-relevant $\iota\!\!\!-$ = 5/9 configuration. The other plates act as baffles to enhance neutral recycling near the target plate, both to increase the plasma density at that point and to promote higher neutral pumping by the titanium getter pumps placed in the divertor subvolume. In addition to H_α, an extensive arsenal of new diagnostics has been prepared to join established core diagnostics in order to document plasma behaviour both upstream near the core plasma and downstream at the target plates. Emphasis is placed on duplication of diagnostics to assess up-down and toroidal asymmetries, as well as a concentration of key diagnostics within one sector [25].
Island divertor experiments on W7-AS will be dictated by experience gained from tokamaks, in addition to preparatory experiments performed on W7-AS using the inboard limiters as

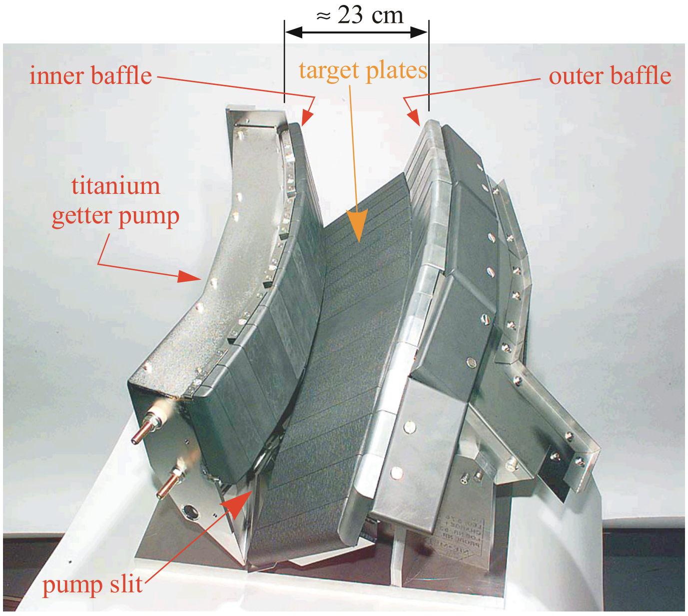

Fig. 4. Island divertor module. In contrast to tokamaks, toroidally discontinuous target plates are used, thus the modules are closed by baffles in the toroidal direction as well. The length is about 70 cm compared with the length of a toroidal field period of 250 cm.

"target plates" [26]. Hereby, edge predictive codes such as EMC3/EIRENE [27] are essential to allow consideration of differences expected to accrue from the stellarator-specific island structure and 3D geometry [6].

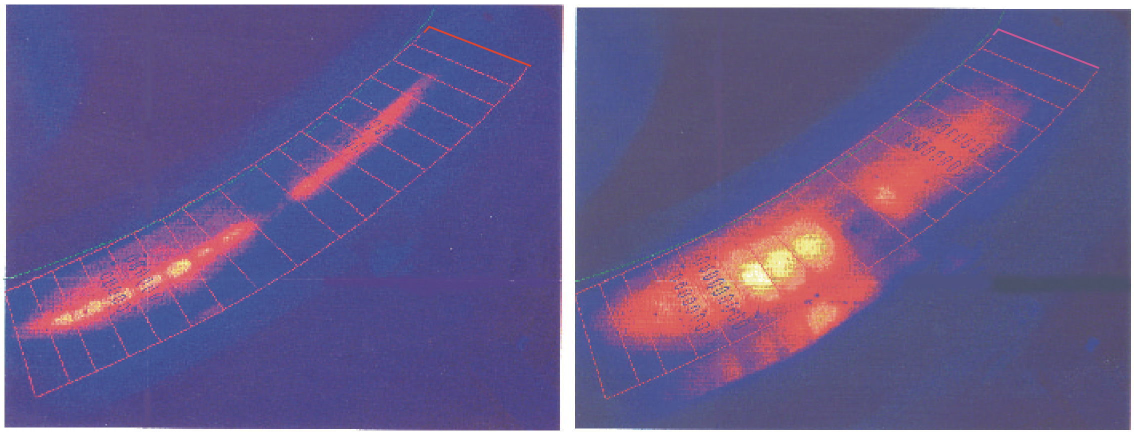

Fig. 5. First measurements of the H_α emission with a divertor-relevant $\iota \approx 5/9$ magnetic field configuration (left) indicate that the plasma-wall interaction takes place essentially along a stripe on the target plates similar to the divertor leg in tokamaks. The gap is the result of modifications for diagnostic access. For comparison a low $\iota = 0.4$ case with smooth flux surfaces is shown on the right. In this case, neutral recycling also takes place on the outer baffle.

To increase flexibility of the edge magnetic structure, 10 control coils were installed already one year ago. These coils (2 per field period) are again resonant to the fivefold toroidal magnetic field symmetry. Therewith, changes in the size of the natural islands as well as in internal shear are possible. Correspondingly, alteration of the upstream-downstream field line connection length L_c permits modification of the ratio between cross-field and parallel transport. Preliminary experiments have demonstrated the feasibility of this technique, whereby a factor of 1.8 increase in L_c resulted in an appropriate broadening of the power deposition profile measured by an IR camera at an inboard limiter [28].

To reduce power loading at the target plates in the next stellarator generation under steady-state conditions, it will be helpful to operate in at least a partially-detached regime at the target plates. EMC3 predictions for W7-AS indicate that with a 1 MW power flow into the scrape-off layer, upstream separatrix densities n_{es} of roughly $8 \cdot 10^{13}$ cm^{-3} are necessary to achieve detachment under the assumption of a carbon sputtering coefficient of 1.5% at the divertor target plates [29,30]. These conditions (1 MW, $8 \cdot 10^{13}$ cm^{-3}) have already been achieved with the inboard limiters, giving reason to believe that with the divertor modules W7-AS will be able to investigate the entire spectrum of target-plasma conditions relevant to future operations [26].

5. High Confinement Discharges at high Iota

The natural islands on W7-AS are advantageous in the case of an island divertor, but they deteriorate plasma confinement in the range of high rotational transform $\iota\!\!\!- > 0.45$ mainly due to a restriction of the effective plasma cross section. However, by means of the control coils the size of the islands can be changed (Fig. 6), and their effect on plasma confinement studied. Based on vacuum field predictions for the effective plasma radius a_{eff}, roughly a dependence of the diamagnetic energy content $W_{dia} \propto a_{eff}^2$ was found [26] at constant average density, which is close to that expected from the W7-AS scaling law [31]. Also, the variation of the plasma radius was clearly seen in electron temperature profiles measured by ECE [28].

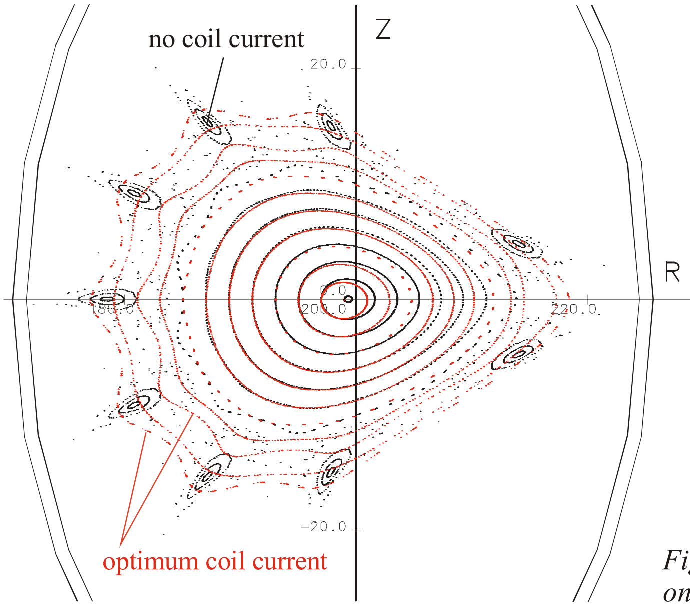

Fig. 6. Compensation of natural islands on W7-AS by means of the control coils.

Thus an interesting application of the control coils was the comparison of high confinement discharges at $\iota\!\!\!- > 1/3$, where they were initially established, with the high iota range $\iota\!\!\!- > 1/2$ with compensated natural islands. The discharges are distinguished by confinement times about a factor of 2 above the W7-AS scaling law [31] and have been obtained for two heating scenarios. The first, with combined ECRH and NB heating, is characterized by high central electron and ion temperatures [32], and the other, with low power NB heating (just one source) at the highest possible density (up to about $1.5 \cdot 10^{14}$ cm^{-3}) [33], by $\tau_E > 60$ ms, the highest energy confinement times obtained so far on W7-AS. Besides low wall recycling, especially in the latter case very low impurity radiation is mandatory.

In fact, for these discharges similar plasma performance (W_{dia}, electron temperature) could be achieved at low iota and at high iota with edge islands compensated but the long pulse behaviour was still different (Fig. 7). At $\iota\!\!\!- > 1/2$ the energy content decreased faster in time (at $\iota\!\!\!- > 1/3$ almost stationary discharges up to 1.8 s could be produced), probably due to the faster

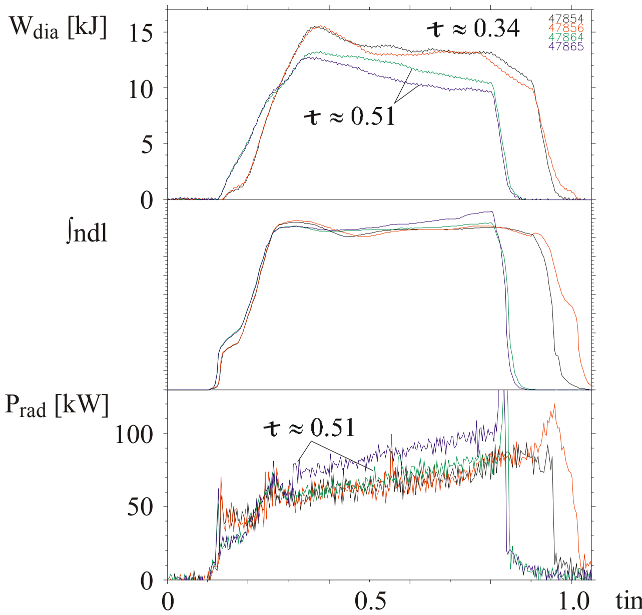

Fig. 7. Diamagnetic energy content, line density and radiation power of high confinement discharges with 350 kW co-NB heating at 2.5 T for ι *close to 1/3 and 1/2 where edge islands are compensated. Average density is above* $1\cdot10^{14}$ cm^{-3}.

increasing impurity radiation. The remaining difference could be caused by differences in the magnetic field structure at the plasma boundary. At $\iota > 1/3$ flux surfaces are smooth everywhere, equivalent to very long magnetic field connection lengths, whereas in the high iota case only the fundamental multipole component of the magnetic perturbation field can be compensated. The edge structure still remains somewhat deformed partly with short connection lengths to arbitrary positions in the torus (Fig. 6) so that it is difficult to control the plasma wall interaction sufficiently well and to avoid enhanced impurity radiation. With the divertor modules this long time behaviour should be improved further, although the plasma radius is generally reduced by about 10%.

6. A new H-mode Window

In the experimental campaign following the installation of the control coils a new H-mode window on the ι-scale was discovered at $\iota(a) \approx 0.56$ during the plasma edge studies. Like the two previously reported operational windows, the magnetic field configuration at the plasma edge is characterized by an island separatrix being within (at $\iota(a) \approx 5/9$) or close to the limiters (at $\iota(a) \approx 10/19$ or $10/21$) [34]. Besides the specific edge magnetic field configuration (mixture between magnetic separatrix and materially limited plasma) viscous damping of the poloidal plasma flow may also be important [35].

The existence range of the H-mode was studied in density ramp discharges at constant heating power (Fig. 8). The threshold density $\overline{n}_e^{thr}$ for the transition to the H-mode is usually not much smaller than the density limit in low power NB heated discharges or compared with the cutoff density in the case of ECRH ($n_e < 1.2\cdot10^{14}$ cm^{-3}). Especially in the new ι window a rather distinct improvement of confinement was found in NB heated discharges with a gain in energy confinement time up to a factor of 1.6 after the transition to an ELM free H*-mode. As in tokamaks, H*-scenarios are found to be transient. The improvement of the particle confinement results in a loss of the density control followed rather rapidly by a radiative density limit (Fig. 8).

Further information was obtained during these experiments on the phenomena before or during the H-mode transition (e.g. a quasi-continuous change in ELM behaviour), on the scaling

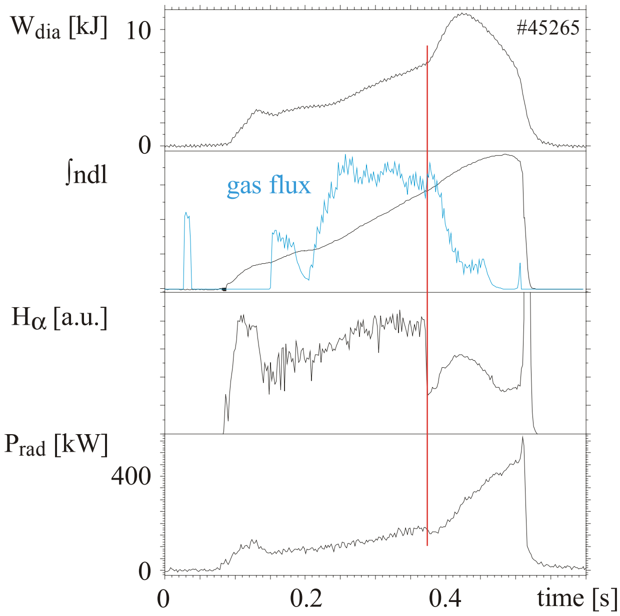

Fig. 8. Diamagnetic energy content, line density and radiation power of an H-mode discharge with 350 kW co-NB heating at 2.5 T and $\iota \approx 0.56$. Maximium density is about $1.5 \cdot 10^{14}$ cm^{-3}. After the transition to an ELM-free H-mode, indicated by the drop of the H_α signal, density control is lost.*

with NB heating power and on changes in edge parameters and gradients [34,36]. Comparing these results to findings on tokamaks some differences are indicated: the threshold density for the H-mode transitions increases with power, $\bar{n}_e^{thr} \propto P$ (varying the constant heating power from shot to shot), and not the reverse, $P^{thr} \propto \bar{n}_e$, as known from tokamaks. In [36] this behaviour is related to edge parameters, in particular to the dependence of the ion temperature gradient and hence the gradient of the radial electric field on density and heating power.

This can be an important result with respect to the divertor experiments since the new H-mode ι-window is almost identical to the ι-window for the divertor experiments ($\iota(a) \approx 5/9$). However, to achieve plasma detachment in the divertor, high edge densities are necessary whereas edge densities are typically low during the H*-mode [34,37]. On the other hand, high edge densities require high NB heating power where n_e^{thr} for the transition to the H*-mode increases, whereby bursts of ELMs or quasi-periodic ELMs (with similarities to type III ELMs in tokamaks) are often observed, leading to increased edge densities under almost stationary conditions. Such a transition to an ELMy H- mode or even L-mode could represent an acceptable core-edge compromise for future divertor experiments, if sufficiently high densities at the separatrix can be established [26].

7. Disruption-like Phenomena on W7-AS at finite toroidal current

The goal of the optimized stellarator line at IPP is to find a stellarator fusion reactor solution where all requirements are fulfilled simultaneously at least sufficiently well. Of course, better solutions for individual properties can exist. In particular, it is an important demand for an optimized magnetic field configuration that all pressure driven plasma currents remain small in order not to perturb this configuration. As a consequence there is no energy potential for plasma current driven instabilities even at high β-values, and current disruptions cannot occur. On the other hand, a toroidal plasma current provides a simple method to produce the rotational transform necessary for magnetic confinement. Within the flexibility of stellarator configurations it is also possible to maximize the bootstrap current and to increase in this way a rather small external rotational transform [38].

On W7-AS the bootstrap current is rather large (tokamak-like). Additional ohmic currents can

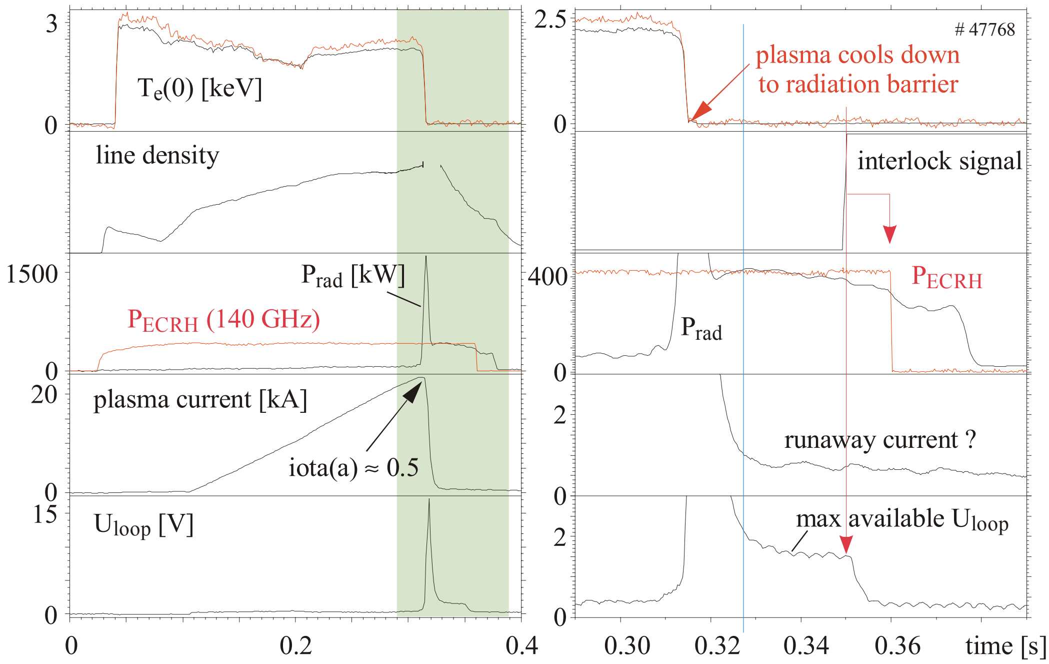

Fig. 9. Disruption-like event on W7-AS caused by rapidly growing tearing modes (not shown) during a rather steep current-ramp experiment (B_O = 2.5 T, $<n_e>\approx 4\times10^{13}$ cm^{-3}). On the right it can be seen that the ECE electron temperature is quenched within about 1 ms. At these low temperatures, the available loop voltage is not sufficient to maintain the plasma current. The discharge is terminated by an interlock signal switching off the ECRH at very small energy content. At constant vertical field the hoizontal plasma shift is limited to $\Delta r/a$ < 10% for a plasma current corresponding to $q(a)\approx$ 6.

be induced by means of the ohmic heating transformer. In this way the stability against toroidal current driven instabilities can be studied up to tokamak-like currents, but at a rather high external rotational transform of $\iota > 0.3$ at $B_O = 2.5$ T. The external poloidal fields are fixed in space and have a twofold effect. Firstly, they change the relative position of resonant magnetic surfaces with respect to the plasma current distribution, which helps especially in the case of ohmic heating alone to stabilize tearing modes [39]. Secondly, they always provide a plasma equilibrium in the sense that horizontal displacements of the plasma due to changes in plasma pressure or toroidal currents are usually small as compared with the plasma radius.

In order to generate disruption-like phenomena on W7-AS the plasma current (sum of bootstrap and OH current) is ramped up rather quickly (Fig. 9). An electron cyclotron resonance heated (ECRH) "target" plasma is used so that the ohmic heating is a negligible fraction of the total heating power because of the high electron temperatures. The toroidal current produces magnetic shear (its effect on confinement is discussed in Ref. [40,41]), and, in addition, is an energy source that can drive instabilities. The positional stability of the plasma is demonstrated by the fact that the vertical field is kept constant throughout the discharge. If the total rotational transform ι (a) (external plus OH current component) approaches 1/2 at the plasma boundary during the current ramp, quite often bursts of (m=2, n=1) tearing modes occur with some intermediate deterioration of the plasma confinement. More details together with the results of Δ'-code stability calculations can be found in [15,42,43].

Sometimes the amplitudes of (2,1) tearing modes attain such large values that the electron temperature cools down to some 10 eV within about 1 ms, and consequently the plasma current is quenched. At these low temperatures the total heating power is radiated away, whereas the density decays on a 30 ms time scale. The discharge is terminated only when the heating power is switched off (Fig. 9). With sufficient heating power or at lower densities it would be possible to overcome the radiation barrier and to heat up the plasma again. With combined ECRH and NB heating, pure bootstrap currents (augmented by NB driven currents due to co-injection) up to 20 kA could be achieved slowly rising according to their L/R time constant of about 1 s. In this case, only a minor reaction on plasma confinement was observed for $\iota(a) \approx 1/2$ [15,43].

8. Future Prospects

After installation of the divertor modules and improvement of the NB heating system the last experimental period on W7-AS has now been started before the permanent shutdown scheduled for summer 2002. Essential goals are to test once more the operational boundaries with respect to the high β-limit and the density limit and to check plasma performance in high confinement and H-mode discharges in the presence of an island divertor. The divertor program itself aims to evaluate basic elements of the island divertor concept foreseen for W7-X in order to experimentally examine the optimization tools used for the design of W7-X as complete as possible within the technical constraints given by W7-AS.

References

[1] GRIEGER, G., et al., "Physics optimization of stellarators", Physics of Fluids **B4** (1992) 2081.
[2] WOBIG, H., et al., "The theoretical basis of a drift optimized Stellarator reactor", Plasma Phys. Control. Fusion **35** (1993) 903.
[3] RENNER, H., et al., Plasma Phys. Control. Fusion **31** (1989) 1579.
[4] SAPPER, J., et al., Fusion Technol. **17** (1990) 62.
[5] Wanner, M. and the W7-X Team, "Design goals and status of the W7-X project, http://hsxa.ece.wisc.edu/Stell_workshop/four-pag.htm.
[6] WAGNER, F., et al., "Overview on W7-AS results with relevance for W7-X and the low shear stellarator line", Fusion Energy 1998 (Proc. 17th Int. Conf. Yokohama, 1998), IAEA, Vienna (1999) (CD-ROM file OV2/4).
[7] RENNER, H., et al, Proc. 19th EPS Conf. on Contr. Fusion. and Plasma Physics (Innsbruck) 16C Part I, (1992) 501.
[8] KICK, M., et al., Plasma Physics and Controlled Nuclear Fusion Research, (Proc. 16th Int. Conf. Montreal, 1996) Vol. 2 (1997) 27.
[9] ERCKMANN, V., et al., Plasma Physics and Contr. Fusion **34** (1992) 1917.
[10] HARTMANN, D., et al., Proc. 27th EPS Conf. on Contr. Fusion. and PlasmaPhysics (Budapest) 2000, http://bilbo.rmki.kfki.hu/pdf/ (file OR 002).
[11] LAQUA; H., et al., Proc. 26th EPS Conf. on Contr. Fusion. and Plasma Physics (Maastricht) (1999) (CD-ROM file p4053).
[12] MAASSBERG, H., et al., "High power ECCD experiments at W7-AS", this conference, EXP4/04.
[13] NUEHRENBERG, C., Phys. Plasmas **6** (1999) 137.
[14] GEIGER. J., et al., Proc. 23th EPS Conf. on Contr. Fusion. and Plasma Physics (Kiev) 20C Part II, (1996) 491.
[15] WELLER, A., et al., "Survey of MHD Instabilities in the W7-AS stellarator", submitted to Physics of Plasmas
[16] JAENICKE, R., et al, Plasma Phys. Control. Fusion **37**(11A) (1995) A163.
[17] WELLER, A., et al., Fusion Energy 1998 (Proc. 17th Int. Conf. Yokohama, 1998), IAEA, Vienna (1999) (CD-ROM file EX2/1).

[18] PENNINGSFELD, F.P., et al., Proc. 23th EPS Conf. on Contr. Fusion. and Plasma Physics (Kiev) 20C Part II, (1996) 483.
[19] GIANNONE, L., et al., Plasma Physics and Contr. Fusion **42** (2000) 603.
[20] GIANNONE, L., et al., Proc. 27th EPS Conf. on Contr. Fusion. and PlasmaPhysics (Budapest) 2000, http://bilbo.rmki.kfki.hu/pdf/ (file P3 079).
[21] BORRASS, K., et al., Nucl. Fusion **33** (1993) 63.
[22] ITER Physics Basis, publ. in Nucl. Fusion **39** (12) (1999), Chapter 3, p 2316.
[23] KISSLINGER, J., et al., Proc. 22th EPS Conf. Contr. Fus. Plasma Phys. (Bournemouth), Vol. 19C, part III, (1995) 149.
[24] SARDEI, F., et al., J. Nucl. Mater. **241-243** (1997) 135.
[25] McCORMICK, K., "Edge Diagnostic Overview for the W7-AS Divertor-Phase", http://hsxa.ece.wisc.edu/Stell_workshop/four-pag.htm.
[26] McCORMICK, K., et al., Plasma Phys. and Contr. Fusion 41 (1999) B285.
[27] FENG, Y., et al., J. Nucl. Mater. **266-269** (1999) 812.
[28] KOENIG, R.W.T., et al., "Island divertor investigations on the W7-AS stellarator", Proc. 14th Int. Conf. on Plasma Surface Interactions, Rosenheim, Germany (2000), accepted for publication in J. Nucl. Mater.
[29] FENG, Y., private communucation
[30] SARDEI, F., et al., "Island divertors: Concepts and status of experimental and modelling results", this conference, EXP4/28
[31] STROTH, U., et al., Nucl. Fusion **36** (1996)1063.
[32] KICK, M., et al., Plasma Phys. Control. Fusion **41** (1999) A549.
[33] STROTH, U., et al., Plasma Phys. Control. Fusion **40** (1998) 1551.
[34] HIRSCH, M., et al., Plasma Phys. Control. Fusion **42** (2000) A231.
[35] WOBIG, H., KISSLINGER, J., Proc. 24th EPS Conf. on Contr. Fusion. and Plasma Physics (Berchtesgaden) 21A Part IV, (1997) 1669.
[36] GRIGULL, P., et al., "Edge transport barrier formation and ELM phenomenology in the W7-AS stellarator", Proc. 14th Int. Conf. on Plasma Surface Interactions, Rosenheim, Germany (2000), accepted for publication in J. Nucl. Mater.
[37] McCORMICK, K., et al., "On the way to Divertor detatchment in the W7-AS stellarator", Proc. 14th Int. Conf. on Plasma Surface Interactions, Rosenheim, Germany (2000), accepted for publication in J. Nucl. Mater.
[38] REIMANN, A., et al., Plasma Phys. Control. Fusion **41** (1999) B273.
[39] WVII-A Team, Nucl. Fusion **20** (1980) 1093.
[40] ERCKMANN, V., et al., Plasma Physics and Controlled Nuclear Fusion Research (Proc. 16th Int. Conf. Montreal, 1996) Vol. 2 (1997) 119.
[41] BRAKEL, R., et al., Proc. 25th Eur. Conf. on Controlled Fusion and Plasma Physics (Prague) 1998 (CD-ROM file B006pr), http://www.ipp.cas.cz/conference/98icpp/.
[42] WELLER, A., et al., "Effects of toroidal currents upon magnetic configurations and stability in W7-AS", this conference, EX7/4.
[43] SALLANDER, E., WELLER, A., W7-AS Team, Nucl. Fusion **40** (2000) 1499.